

Genetics and evolution of ultraviolet vision in vertebrates

Shozo Yokoyama*, Yongsheng Shi

Department of Biology, Syracuse University, 130 College Place, Syracuse, NY 13244, USA

Received 12 October 2000; revised 13 November 2000; accepted 14 November 2000

First published online 23 November 2000

Edited by Matti Saraste

Abstract Various vertebrates use ultraviolet (UV) vision for such basic behaviors as mating, foraging, and predation. We have successfully interchanged the color-sensitivities of the mouse UV pigment and the human blue pigment by introducing forward and reverse mutations at five sites. This unveils for the first time the general mechanism of UV vision. Most contemporary UV pigments in vertebrates have maintained their ancestral functions by accumulating no more than one of the five specific amino acid changes. The avian lineage is an exception, where the ancestral pigment lost UV-sensitivity but some descendants regained it by one amino acid replacement at an entirely different site. © 2000 Federation of European Biochemical Societies. Published by Elsevier Science B.V. All rights reserved.

Key words: Ultraviolet visual pigment; Opsin; Absorption spectrum; Molecular evolution; Vertebrate

1. Introduction

Many flowers have ultraviolet (UV) markings that guide the visiting insects toward nectar or pollen [1]. Similarly, the petals of bird-pollinated flowers have substantial UV reflectance, which provides attractive targets to birds with UV vision [2]. Scales of fish and feathers of birds often reflect UV, enhancing the visibility of their body coloration patterns [3,4]. Indeed, many fishes, amphibians, reptiles, birds, and mammals use UV vision for such basic activities as foraging and mating [2,5–8]. UV vision is achieved through a class of cone photoreceptors containing UV pigments that absorb light maximally (λ_{\max}) at about 360–370 nm [8]. Despite its biological importance, the mechanism of spectral tuning in UV pigments remains mostly an area of speculation. The visual pigments consist of the chromophore, either 11-*cis*-retinal or 11-*cis*-3,4-dehydroretinal, and a transmembrane protein, opsin. All currently known UV pigments belong to a specific evolutionary group of pigments, often referred to as the short wavelength-sensitive type 1 (SWS1) group, while violet pigments (λ_{\max} = 395–430 nm) belong either to the SWS1 group or to a paralogous SWS2 group [9–11].

The molecular mechanisms of color vision can be elucidated in two steps [9–14]. First, we need to identify potentially important amino acid changes that may shift the λ_{\max} values of visual pigments. Second, these amino acid changes have to be tested whether they are in fact responsible for the λ_{\max} -shifts using site-directed mutagenesis and cultured cells [15]. Here,

through a series of mutagenesis experiments using the mouse UV pigment and the human blue (or violet) pigment, we have identified five amino acids that characterize the absorption spectra of UV pigments in vertebrates. Using statistical inference on the amino acid sequences of visual pigments in ancestral vertebrates, we will also show a remarkably simple rule of the evolution of UV and related pigments.

2. Materials and methods

2.1. Regeneration of visual pigments, site-directed mutagenesis, and spectral analyses

The SWS1 opsin cDNA clones of the mouse (*Mus musculus*) and goldfish (*Carassius auratus*) have been obtained in our laboratory [16], while that of the human is a gift from Dr. Jeremy Nathans at the Johns Hopkins University, Baltimore, MD, USA. Mutants of these cDNA clones were generated by using QuickChange site-directed mutagenesis kit (Stratagene). All cDNA fragments that were subjected to mutagenesis were sequenced to rule out spurious mutations, by subcloning the mutant clones into pBluescript SK(–) vector and sequencing by cycle sequencing reactions using the Sequitherm Excel II Long-Read kits (Epicentre Technologies, Madison, WI, USA) with dye-labeled M13 forward and reverse primers. Reactions were run on a LI-COR 4200LD automated DNA sequencer (LI-COR, Lincoln, NE, USA). The mutants were then subcloned into the expression vector pMT5. These plasmids were expressed in COS1 cells by transient transfection. The visual pigments were regenerated by incubating with 11-*cis*-retinal (Storm Eye Institute, Medical University of South Carolina). These pigments were purified using immobilized 1D4 (The Cell Culture Center, Minneapolis, MN, USA) in buffer consisting of 50 mM *N*-(2-hydroxyethyl) piperazine-*N'*-2-ethanesulfonic acid (pH 6.6), 140 mM NaCl, 3 mM MgCl₂, 20% (wt/vol) glycerol, and 0.1% dodecyl maltoside [15]. UV visible absorption spectra of the visual pigments, obtained through the in vitro assay, were recorded at 20°C, using a Hitachi U-3000 dual beam spectrophotometer. Visual pigments were also bleached by a 366 nm UV light illuminator and a 60 W room lamp with 440 nm cut-off filter and denatured by sulfuric acid (H₂SO₄) at pH 1.8 in the dark separately. Recorded spectra were analyzed using SigmaPlot software (Jandel Scientific, San Rafael, CA, USA).

2.2. Sequence data analyses

Previously, we have studied the phylogenetic relationships of goldfish (*C. auratus*; P359), zebrafish (*Danio rerio*; P362), clawed frog (*Xenopus laevis*; P425), chicken (*Gallus gallus*; P415), pigeon (*Columba livia*; P393), parakeet (*Melopsittacus undulatus*; P371), zebra finch (*Taeniopygia guttata*; P358), canary (*Serinus canaria*; P366), chameleon (*Anolis carolinensis*; P358), human (*Homo sapiens*; P414), macaque (*Macaca fascicularis*; P430), squirrel monkey (*Saimiri boliviensis*; P430), marmoset (*Callithrix jacchus*; P423), mouse (*M. musculus*; P359), and rat (*Rattus norvegicus*; P358) pigments, where the numbers after P refer to λ_{\max} values [14]. Today, two additional pigments are available: Malawi fish (*Metriacalma zebra*; P368) (GenBank accession number AF191220) and bovine (*Bos taurus*; P431) (U92557). In order to construct a rooted phylogenetic tree of these 17 pigments and infer the amino acid sequences of ancestral organisms, bovine (P500), goldfish (P511), goldfish (P441), chameleon (P437), goldfish (P559), clawed frog (P611), chameleon (P561), pigeon (P558), and human (P560) pig-

*Corresponding author. Fax: (1)-315-443 2012.
E-mail: syokoyam@mailbox.syr.edu

ments were used as the outgroup [14]. Note that the λ_{\max} values of the goldfish (P359), chicken (P415), pigeon (P393), zebra finch (P358), chameleon (P358), human (P414), bovine (P431), mouse (P359), and rat (P358) pigments have been determined by the in vitro assay in our laboratory. The λ_{\max} values of the clawed frog (P425) and parakeet (P371) pigments are determined by the in vitro assay and those of the remaining six pigments by microspectrophotometry and electroretinogram (see [11]).

To construct a phylogenetic tree of these pigments, the number (K) of amino acid replacements per site for a pair of sequences was estimated by $K = -\ln(1-p)$, where p is the proportion of different amino acids per site. The numbers of nucleotide substitutions per site were also estimated by using Kimura's formula [17]. Topology and branch lengths of the phylogenetic tree were evaluated by using the neighbor-joining (NJ) method [18]. The reliability of the NJ tree topology was evaluated by the bootstrap analysis with 1000 replications [19].

The ancestral amino acid sequences of the pigments were inferred by a likelihood-based Bayesian method [20] using a modified version of the Jones, Taylor and Thornton (JTT) model [21], the Dayhoff model [22], and the equal-input model. In the equal-input model, we assume that the amino acid change from one amino acid (i) to another (j) is proportional to the frequency of amino acid (j) in the sequence.

3. Results and discussion

3.1. Comparison of the amino acid sequences of mammalian and chameleon SWS1 pigments

When the amino acid sequences of the SWS1 pigments are compared site by site, we see that no amino acid is restricted to the UV pigments. This shows that the absorption spectra of the UV pigments in various vertebrates have been achieved by different mechanisms. Indeed, in the avian species, the UV pigments evolved from the violet pigments by a single amino acid replacement, S90C, where the amino acid number corresponds to that of the bovine rhodopsin [14,23]. However, since none of the other UV pigments has C90, it is clear that the UV pigments in the birds and those in the other vertebrate species have evolved by entirely different mechanisms.

	I	II	III	VI	VII	
	1	1	1	2	2	3
	4	4	5	8	9	9
	6	9	2	6	3	7
				4	8	9
				1	3	8
				0	0	0
Chameleon (P358)	F	F	T	F	T	A
Human (P414)	T	L	F	L	P	A
Macaque (P430)	T	L	F	L	P	N
Squirrel monkey (P430)	I	L	L	L	P	N
Marmoset (P423)	I	L	L	L	P	N
Bovine (P431)	F	F	T	Y	I	T
Mouse (P359)	F	F	T	F	T	A
Rat (P358)	F	F	T	F	T	A

Fig. 1. Variation at the UV pigment-specific amino acid sites. The number after P in the parentheses refers to λ_{\max} . The UV pigments are boxed. I–VII indicate seven transmembrane helices [29]. The amino acid site numbers are those of the bovine (P500) pigment.

In order to identify potentially important amino acids that characterize the absorption spectra of UV pigments of the non-avian vertebrates, we compared the amino acid sequences of the SWS1 pigments of chameleon and mammals site by site. We can then identify 13 sites where amino acids are conserved among the UV pigments, but they are different from those of most violet pigments (Fig. 1). From this comparison, we hypothesize that if there exists any common molecular basis of the UV-sensitivity among non-avian vertebrates, then some of these amino acid differences must be responsible for the differentiation of the UV and violet pigments.

3.2. Absorption spectra of the mouse and human SWS1 pigments

We have reconfirmed the λ_{\max} values of the human blue (or violet) pigment [24] and the mouse UV pigment [16] to be 414 nm and 359 nm, respectively. We have constructed a chimeric pigment, consisting of the amino acids 1–146, including the transmembrane helices I–III, of the human blue pigment and the amino acids 147–348, including the helices IV–VII, of the mouse UV pigment. This pigment attains a λ_{\max} value at 411 nm. On the other hand, the pigment with the helices I–III of the mouse pigment and the helices IV–VII of the human pigment gives a λ_{\max} value at 359 nm (results not shown). These observations demonstrate that the UV- and violet-sensitivities are determined mostly by the amino acid differences on the transmembrane helices I–III.

When four amino acid changes F86L/T93P/A114G/S118T are introduced into the helices II and III of the mouse pigment, where the amino acid site numbers are those of the bovine (P500) pigment, the mutant pigment gives a λ_{\max} value at 400 ± 1 nm (dark, Fig. 2A). When F46T, F49L, T52F, and F46/T52F on the helix I are added separately into the mouse mutant pigment already containing F86L/T93P/A114G/S118T, the four new pigments attain λ_{\max} values at 403 ± 2 nm, 404 ± 2 nm, 407 ± 1 nm, and 406 ± 1 nm, respectively (dark, Fig. 2B–E). Thus, among the three amino acid changes on the helix I, T52F is the most effective in shifting the λ_{\max} value into violet.

It should be noted that when these regenerated pigments are exposed to light, new absorption peaks at ~ 380 nm are achieved (light, Fig. 2A–E), which are explained by all-*trans*-retinal having dissociated from opsin [25]. Furthermore, when these pigments are denatured by sulfuric acid (H_2SO_4), the new peaks at ~ 440 nm appear (acid, Fig. 2A–E), which are explained by protonated Schiff base 11-*cis*-retinal free in solution [26]. These two control experiments demonstrate that the peaks at the UV–violet region in Fig. 2A–E are indeed due to the mutant visual pigments. Note, however, that the absorption spectra of the mutant pigments in Fig. 2A–E are somewhat broader than that of the wild-type mouse UV pigment. A similar observation has been made for the zebra finch UV pigment with C90S [13]. The absorption spectrum of this mutant pigment cannot be narrowed even when it is subjected to various pH conditions ranging from 4.4 to 11.3 [13]. At present, it is not clear why the absorption spectra of this and the mutant pigments in Fig. 2A–E are broader than those of the wild-type pigments. Thus, the λ_{\max} values in Fig. 2 need to be interpreted with caution. However, it is clear that the mouse UV pigment with T52F/F86L/T93P/A114G/S118T is not UV-sensitive any more (Fig. 2D). The amino acid changes

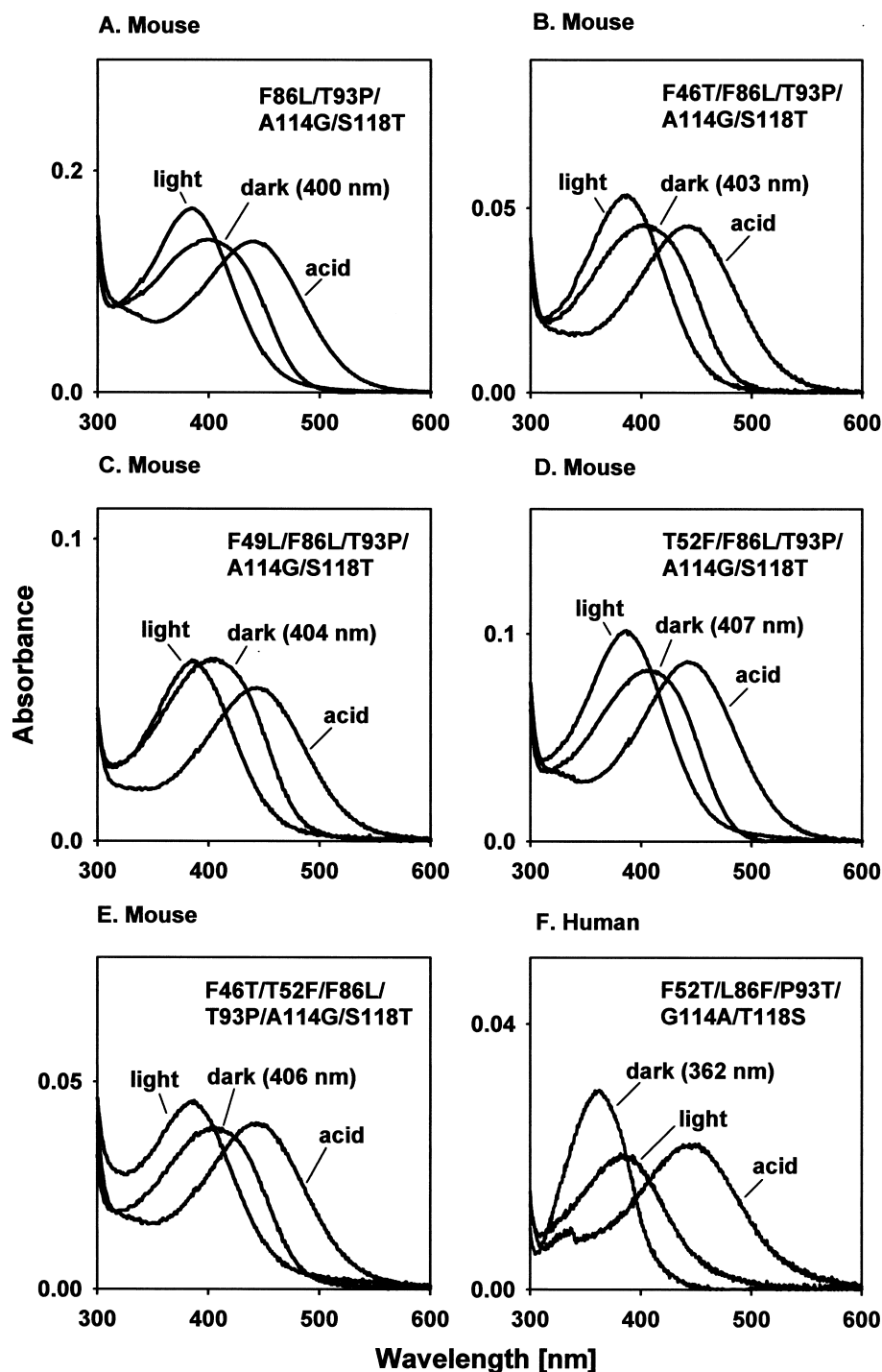


Fig. 2. Absorption spectra for the mouse UV pigment and the human blue pigment. Absorption spectra of the mouse pigments with (A) amino acid changes F86L/T93P/A114G/S118T, (B) F46T/F86L/T93P/A114G/S118T, (C) F49L/F86L/T93P/A114G/S118T, (D) T52F/F86L/T93P/A114G/S118T, and (E) F46T/T52F/F86L/T93P/A114G/S118T and those after exposure to light (light) and H_2SO_4 (acid), where the amino acid numbers are those of the bovine (P500) pigment. F: Absorption spectrum of the human pigment with F52T/L86F/P93T/G114A/T118S and those after exposure to light and H_2SO_4 .

at these five sites explain $\sim 90\%$ of the λ_{max} -shift from the mouse UV pigment to the human blue pigment. Importantly, when the reverse mutations are introduced into the human blue pigment, the mutant pigment achieves a λ_{max} value at 362 ± 1 nm, explaining 95% of the difference (dark, Fig. 2F).

These mutagenesis results show that the molecular basis of the differentiation of the UV and violet pigments can be elu-

cidated by studying the amino acid differences at sites 52, 86, 93, 114, and 118. These sites are all located in the transmembrane helices of the pigments (Fig. 1), where most interactions between the chromophore and an opsin must occur [9–11,24,27,28]. In a tertiary structure, these five sites are positioned near the Schiff base nitrogen, the counterion E113 of the Schiff base, and K296 [29]. Thus, the amino acid changes

at these sites must introduce a significant change in the pigment structure and in the nature of the interaction between the opsin and chromophore.

3.3. Phylogenetic relationships of the SWS1 pigments

When the NJ method is applied to the amino acid sequences, the 17 SWS1 pigments are classified into five groups with the phylogenetic relationship of (fish pigments, (clawed frog pigment, ((chameleon pigment, bird pigments)₆₀, mammalian pigments)₈₀)₁₀₀)₁₀₀, where each subscript indicates the percent bootstrap values. More specifically, we find the phylogenetic relationships of ((goldfish (P359), zebrafish (P362))₁₀₀, Malawi fish (P368))₁₀₀ among the fish pigments; (((canary (P366), zebra finch (P358))₁₀₀, parakeet (P371))₄₃, pigeon (P393))₃₈, chicken (P415))₇₃ among the bird pigments; and (((human (P414), macaque (P415))₁₀₀, (squirrel monkey (P430), marmoset (P423))₁₀₀)₁₀₀, (bovine (P431), (mouse (P359), rat (P358))₁₀₀)₇₇)₉₈ among the mammalian pigments.

Some of these bootstrap values are not high, but the phylogenetic relationships of the fish, frog, chameleon, bird, and mammalian pigments are consistent with the organismal tree. Among the avian pigments, only the cluster of the zebra finch and canary pigments is reliable (see also [14]). Similarly, the exact phylogenetic position of bovine (P431) pigment among

the mammalian pigments cannot be determined. When the nucleotide sequences of the corresponding opsin genes are used, the reliability of the phylogenetic relationships of the bird pigments does not improve. Furthermore, the bovine (P431) pigment now clusters with the primate pigments rather than with the murine pigments (bootstrap value of 0.91). Fig. 3 shows the composite phylogenetic tree of the 17 SWS1 pigments, which is consistent with the tree topologies based on more extensive molecular data sets [30–32].

3.4. Molecular evolution of the vertebrate SWS1 pigments

Using the JTT, Dayhoff, and equal-input models of amino acid replacements, we inferred the amino acid sequences of the pigments at all interior nodes of the composite phylogenetic tree for the SWS1 pigments in vertebrates (Fig. 3). All three models predict that the amino acid composition at the five critical sites in the ancestral pigment is given by T52/F86/T93/A114/S118, all of which have posterior probabilities higher than 0.90. These amino acids are identical to those of the extant chameleon, mouse, and rat UV pigments. Thus, it is tempting to conclude that the ancestral pigment was a UV pigment. However, this conclusion is premature because T93Q occurred in the ancestor of the three extant fish UV pigments (Fig. 3). Malawi fish UV pigment has an additional

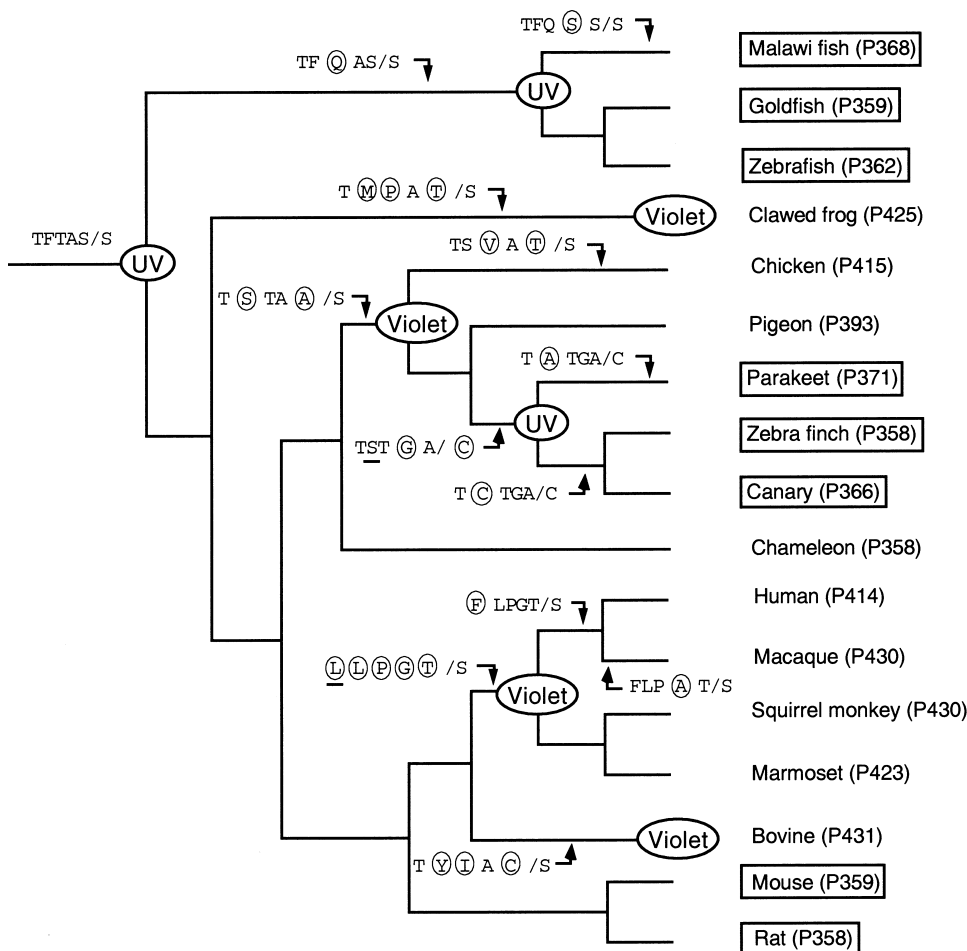


Fig. 3. A composite tree topology of the vertebrate SWS1 pigments and ancestral amino acids inferred by using the JTT and Dayhoff models of amino acid replacement. The UV pigments are boxed. The two ancestral amino acids with probabilities of 90% or less are underlined. The first five amino acids next to the branches are those at sites 52, 86, 93, 114, and 118, in that order, while the sixth amino acids after a slash (/) are those at site 90, where the site numbers are those of the bovine (P500) pigment. The circles indicate amino acid replacements.

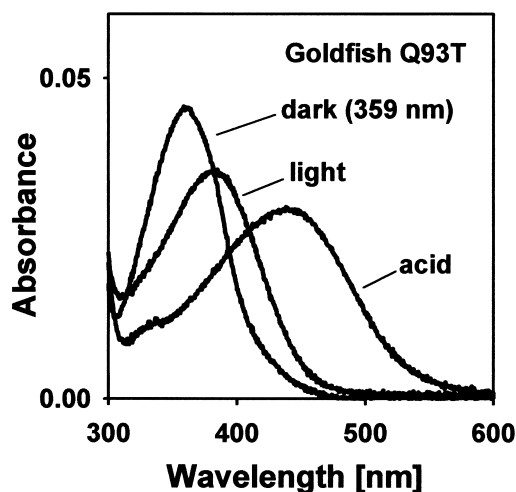


Fig. 4. Absorption spectrum of the goldfish UV pigment with the amino acid change Q93T (dark) and those after exposure to light (light) and H_2SO_4 (acid).

amino acid replacement, A114S. This change is probably not important in the differentiation of the two types of pigments because the three fish pigments have λ_{max} values of 360–370 nm.

In order to determine the λ_{max} value of the pigment in the vertebrate ancestor, it is necessary to evaluate the effect of T93Q on the λ_{max} -shift in the ancestral fish pigment. When the reverse change, Q93T, is introduced into the goldfish UV pigment, the λ_{max} value of the mutant pigment is 358 ± 1 nm which is practically identical to that of the wild-type pigment (Fig. 4). Again, the exposures to light and acid show that this λ_{max} value is due to the mutant visual pigment. Given the importance of site 93 in the spectral tuning of the UV pigments, this result is totally unexpected. Interestingly, when amino acid changes T52F, F86L, T93P, A114G, and S118T are introduced separately into the mouse UV pigment, none of the λ_{max} values of these five mutant pigments is shifted from ~ 360 nm (result not shown). However, as we saw earlier, these five amino acid changes together shift the λ_{max} value ~ 50 nm into violet (Fig. 2D), exhibiting strong synergism among them. This non-linear effect is in sharp contrast to the additive effects of the amino acid changes detected among the red- and green-sensitive pigments [33,34]. The result with the goldfish mutant strongly supports the idea that the ancestral pigment indeed had UV-sensitivity with a λ_{max} value of ~ 360 nm (Fig. 3). Thus, it is most likely that the fish, chameleon, mouse, and rat pigments have maintained their UV-sensitivities by accumulating no more than one of the five specific amino acid changes. On the other hand, most contemporary violet pigments achieved their λ_{max} values by accumulating at least two amino acid changes at these five critical sites. As noted earlier, the avian lineage is an exception to this rule, where the UV pigments have evolved from violet pigments by one amino acid replacement at an entirely different site.

Note that when different estimation procedures are used, the λ_{max} values can differ even for the same pigment. Thus, it is inappropriate to study the mechanisms of spectral tuning in detail using pigments whose λ_{max} values are evaluated using different methods. However, the evolutionary analyses of the

17 pigments in Fig. 3 provide important insights into mechanisms of the spectral tuning in the vertebrate SWS1 pigments. For example, the comparison of the Malawi fish and goldfish pigments may give an impression that one mutation A114S is responsible for the red-shift in the λ_{max} of the former pigment. However, as noted earlier, the mutagenesis results of the goldfish and mouse UV pigments imply that the single mutation should not shift the λ_{max} value of the Malawi fish pigment. These seemingly contradictory observations can be resolved easily by considering that T93Q and A114S in combination, rather than A114S alone, have caused the λ_{max} -shift. Similarly, when the human and macaque pigments are compared, G114A in the latter pigment is associated with the higher λ_{max} value. This λ_{max} -shift makes sense if we consider that the λ_{max} -shift is caused by the interaction between G114A and the four amino acid changes T52F/F86L/T93P/S118T which preceded it. Thus, in order to achieve a wide range of λ_{max} values (360–430 nm), the SWS1 pigments of the non-avian species were required to change at least two of the five amino acids T52, F86, T93, A114, and S118.

In the avian lineage, two amino acid replacements, F86S and S118A, occurred first in the common ancestor (Fig. 3). The amino acid composition at the five critical sites of this ancestral avian pigment is identical to that of the extant pigeon violet pigment and, therefore, this ancestral pigment must have been violet-sensitive with a λ_{max} value at ~ 395 nm (Fig. 3). Then, an amino acid replacement, S90C, shifted the λ_{max} value 20–30 nm toward UV and was the avian ancestor that reinvented a new type of UV pigment [14,23]. In the SWS1 pigment of the primate ancestor, very extensive amino acid replacements appear to have occurred. According to the JTT and Dayhoff models, after its divergence from the bovine pigment, the ancestral primate pigment has undergone the amino acid replacements at all five sites (Fig. 3). At this node, the equal-input model predicts a slightly different pattern of amino acid replacements from those of the other two models: T52F instead of T52L, followed by F52L in the ancestor of the squirrel monkey and marmoset pigments. Being identical to the amino acid composition of the squirrel monkey and marmoset pigments, it is most likely that this ancestral pigment had violet-sensitivity with the λ_{max} value at 420–430 nm. Despite having the same amino acid compositions at the five critical sites, the λ_{max} values of the two violet pigments, both evaluated by microspectrophotometry, differ by 10 nm. To identify the cause of this difference, it is necessary to reevaluate the λ_{max} values of these pigments using the *in vitro* assay and conduct mutagenesis analyses.

Fig. 3 also suggests possible molecular bases of the divergence of the violet pigments. The chicken pigment has a red-shifted λ_{max} value of about 20 nm. This red-shift might have been caused by Y93V and S118T. The squirrel monkey and marmoset pigments have λ_{max} values 10–20 nm higher than the human and macaque pigments. This difference might have been caused by the amino acid difference at site 52. The clawed frog pigment ($\lambda_{\text{max}} = 425$ nm) and the bovine pigment ($\lambda_{\text{max}} = 431$ nm) have amino acid replacements F86M/T93P/S118T and F86Y/T93I/S118C, respectively. These changes may explain most of their red-shifted λ_{max} values measured using the *in vitro* assay, but these possibilities remain to be tested.

Here, the mechanisms of spectral tuning of the SWS1 pigments have been elucidated by the SWS1 pigments based on

11-*cis*-retinal. In nature, some species use 11-*cis*-3,4-dehydroretinal for their visual pigments. The visual pigments with 11-*cis*-3,4-dehydroretinal absorb longer wavelengths than those with 11-*cis*-retinal. Chameleon and goldfish use 11-*cis*-3,4-dehydroretinal as a chromophore almost exclusively and their UV pigments in the native state have λ_{\max} values at 365–370 nm rather than 360 nm (e.g. see [34,35]). Of course, in order to reach the correct molecular bases of the spectral tuning in the UV and violet pigments, we had to consider pigments with the same type of chromophore, 11-*cis*-retinal. In this paper we have identified potentially important amino acid changes that are responsible for the spectral tuning in the SWS1 pigments, providing valuable testable hypotheses on the evolutionary spectral tuning of the pigments. As more SWS1 pigments are characterized for their amino acid sequences and λ_{\max} values, this evolutionary approach will be of increasing value in studying the molecular bases of the differentiation of these various pigments [9–11,27]. In turn, these results will deepen our understanding of the molecular bases of UV vision.

Acknowledgements: We thank J. Belote, P. Dunham, R. Yokoyama, and two anonymous reviewers for their comments on the earlier draft. This work was supported by National Institutes of Health Grant GM42379.

References

- [1] Menzel, R. and Backhaus, W. (1991) in: *The Perception of Colour* (Goura, E.D., Ed.), pp. 262–293, CRC Press, Boca Raton, FL.
- [2] Burkhardt, D. (1982) *Naturwissenschaften* 69, 153–157.
- [3] Harosi, F.I. (1985) in: *The Visual System* (Fein, A. and Levine, J.S., Eds.), pp. 41–55, Liss Press, New York.
- [4] Burkhardt, D. (1989) *J. Comp. Physiol. A* 164, 787–796.
- [5] Viitala, J., Korpimäki, E., Palokangas, P. and Koivula, M. (1995) *Nature* 373, 425–427.
- [6] Bennett, A.T.D., Cuthill, I.C. and Partridge, J.C. (1996) *Nature* 380, 433–435.
- [7] Bennett, A.T., Cuthill, I.C., Partridge, J.C. and Lunau, K. (1997) *Proc. Natl. Acad. Sci. USA* 94, 8618–8621.
- [8] Jacobs, G.H. (1992) *Am. Zool.* 32, 544–554.
- [9] Yokoyama, S. and Yokoyama, R. (1996) *Annu. Rev. Ecol. Syst.* 27, 543–567.
- [10] Yokoyama, S. (1997) *Annu. Rev. Genet.* 31, 315–336.
- [11] Yokoyama, S. (2000) *Prog. Ret. Eye Res.* 19, 385–419.
- [12] Yokoyama, R. and Yokoyama, S. (1990) *Proc. Natl. Acad. Sci. USA* 87, 9315–9318.
- [13] Yokoyama, S., Zhang, H., Radlwimmer, F.B. and Blow, N.S. (1999) *Proc. Natl. Acad. Sci. USA* 96, 6279–6284.
- [14] Yokoyama, S., Radlwimmer, F.B. and Blow, N.S. (2000) *Proc. Natl. Acad. Sci. USA* 97, 7366–7371.
- [15] Yokoyama, S. (2000) *Methods Enzymol.* 315, 312–325.
- [16] Yokoyama, S., Radlwimmer, F.B. and Kawamura, S. (1998) *FEBS Lett.* 423, 155–158.
- [17] Kimura, M. (1980) *J. Mol. Evol.* 16, 111–120.
- [18] Saitou, N. and Nei, M. (1987) *Mol. Biol. Evol.* 4, 406–425.
- [19] Felsenstein, J. (1985) *Evolution* 39, 783–791.
- [20] Yang, Z., Kumar, S. and Nei, M. (1995) *Genetics* 141, 1641–1650.
- [21] Jones, D.T., Taylor, W.R. and Thornton, J.M. (1992) *Comput. Appl. Biosci.* 8, 275–282.
- [22] Dayhoff, M.O., Schwarz, R.M. and Orcutt, B.C. (1978) in: *Atlas of Protein Sequences and Structure* (Dayhoff, M.O., Ed.), Vol. 5, pp. 345–352, National Biomedical Research Foundation, Washington, DC.
- [23] Wilkie, S.E., Robinson, P.R., Cronin, T.W., Poopalasundaram, S., Bowmaker, J.K. and Hunt, D.M. (2000) *Biochemistry* 39, 7895–7901.
- [24] Fasick, J.L., Lee, N. and Oprian, D.D. (1999) *Biochemistry* 38, 11593–11596.
- [25] Mathews, R.G., Hubbard, R., Brown, P.K. and Wald, G. (1963) *J. Gen. Physiol.* 47, 215–240.
- [26] Kito, Y., Suzuki, T., Azuma, M. and Sekoguchi, Y. (1968) *Nature* 218, 955–957.
- [27] Yokoyama, S. (1995) *Mol. Biol. Evol.* 12, 53–61.
- [28] Sakmar, T.P. and Fahmy, K. (1996) *Isr. J. Chem.* 35, 325–337.
- [29] Palczewski, K., Kumasaka, T., Hori, T., Behnke, C.A., Motoshima, H., Fox, B.A., Trong, I.L., Teller, D.C., Okada, T., Stenkamp, R.E., Yamamoto, M., Miyano (2000) *Science* 289, 739–745.
- [30] Cao, Y., Okada, N. and Hasegawa, M. (1997) *Mol. Biol. Evol.* 14, 461–464.
- [31] Shimodaira, H. and Hasegawa, M. (1999) *Mol. Biol. Evol.* 16, 1114–1116.
- [32] Reyes, A., Gissi, C., Pesole, G., Catzeflis, M. and Saccone, C. (2000) *Mol. Biol. Evol.* 17, 979–983.
- [33] Yokoyama, S. and Radlwimmer, F.B. (1998) *Mol. Biol. Evol.* 15, 560–567.
- [34] Yokoyama, S. and Radlwimmer, F.B. (1999) *Genetics* 153, 919–932.
- [35] Kawamura, S. and Yokoyama, S. (1998) *Vis. Res.* 38, 37–44.